

# **Electron Transfer on the Donor Side of Manganese-Depleted Photosystem 2**

ELECTRON TRANSFER IN APO-PS2 COMPLEX

L. A. Vitukhnovskaya<sup>1,2</sup>, E. V. Fedorenko<sup>3</sup>, and M. D. Mamedov<sup>1,a\*</sup>

VITUKHNOVSKAYA et al.

<sup>1</sup>Belozersky Institute of Physico-Chemical Biology, Lomonosov Moscow State University, 119992 Moscow, Russia

<sup>2</sup>Semenov Institute of Chemical Physics, Russian Academy of Sciences, 119334 Moscow, Russia

<sup>3</sup>Moscow Institute of Physics and Technology, 141701 Dolgoprudny, Moscow Region, Russia

<sup>a</sup>e-mail: mahirmamedov@yandex.ru

Received April 10, 2019

Revised June 5, 2019

Accepted June 5, 2019

\* To whom correspondence should be addressed.

*Abbreviations:*  $\Delta\Psi$ , transmembrane electric potential;  $\tau$ , characteristic time; apo-PS2, Mn-depleted PS2 complexes; Chl, chlorophyll; PS2, photosystem 2;  $Q_A$ , primary quinone acceptor; RC, reaction center; WOC, water-oxidizing complex;  $Y_Z$ , tyrosine 161 of the D1 subunit.

**Abstract**—After removal of manganese ions responsible for light-driven water oxidation, redox-active tyrosine  $Y_Z$  (tyrosine 161 of the D1 subunit) still remains the dominant electron donor to the photooxidized chlorophyll  $P_{680}$  ( $P_{680}^+$ ) in the reaction center of photosystem 2 (PS2). Here, we investigated  $P_{680}^+$  reduction by  $Y_Z$  under single-turnover flashes in Mn-depleted PS2 core complexes in the presence of weak acids and  $NH_4Cl$ . Analysis of changes in the light-induced absorption at 830 nm (reflecting  $P_{680}$  redox transitions) at pH 6.0 showed that  $P_{680}^+$  reduction is well approximated by two kinetic components with the characteristic times ( $\tau$ ) of  $\sim 7$  and  $\sim 31$   $\mu s$  and relative contributions of  $\sim 54$  and  $\sim 37\%$ , respectively. In contrast to the very small effect of sodium formate (200 mM), addition of sodium acetate and  $NH_4Cl$  increased the rate of electron transfer between  $Y_Z$  and  $P_{680}^+$  approx. by a factor of 5. The suggestion that direct electron transfer from  $Y_Z$  to  $P_{680}^+$  has a biphasic kinetics and reflects the presence of two different populations of PS2 centers was confirmed by the data obtained using direct electrometrical technique. It was demonstrated that the submillisecond two-phase kinetics of the additional electrogenic phase in the kinetics of photoelectric response due to the electron transfer between  $Y_Z$  and  $P_{680}^+$  is significantly accelerated in the presence of acetate or ammonia. These results contribute to the understanding of the mechanism of interaction between the oxidized tyrosine  $Y_Z$  and exogenous substances (including synthetic manganese-containing compounds) capable of photooxidation of water molecule in the manganese-depleted PS2 complexes.

*Keywords:* photosystem 2, reaction center, apo-PS2, absorption changes, photoelectric response, acetate, ammonia

Light-driven oxidation of water and reduction of plastoquinone in the thylakoid membranes of cyanobacteria and chloroplasts is performed by the photosynthetic reaction center (RC) of photosystem 2 (PS2). The structure of the PS2 complex dimeric form in thermophilic cyanobacteria was determined by X-ray structural analysis with the atomic resolution of 1.9 Å [1-3]. Each PS2 monomer contains 20 protein subunits (molecular weight, 350 kDa), 17 of which are membrane proteins. All main PS2 functional cofactors are located in the integral antenna proteins CP43 and CP47 and in the RC subunits D1 and D2. The water-oxidizing complex (WOC) consisting of the inorganic  $\text{Mn}_4\text{CaO}_5$  cluster and surrounding protein matrix is located at the luminal side of the thylakoid membrane. Note that the three peripheral membrane subunits that interact with the D1/D2 proteins and stabilize the  $\text{Mn}_4\text{CaO}_5$  cluster are located on the RC donor side.

The excitation energy absorbed by the antenna pigments is transferred to the RC, where the charge transfer reactions through the redox cofactors take place. The charge separation between the primary electron donor  $\text{P}_{680}$  and the intermediary electron acceptor pheophytin is stabilized by the electron transfer to the tightly bound plastoquinone  $\text{Q}_A$  followed by  $\text{Q}_A^-$  reoxidation by the secondary quinone acceptor  $\text{Q}_B$ . The redox-active tyrosine residue  $\text{Y}_Z$  (tyrosine 161) of the D1 subunit located between  $\text{P}_{680}$  and WOC links the one-electron photochemical reaction with the four-electron catalytic water oxidation [4-6]. In active PS2,  $\text{Y}_Z$  donates an electron to  $\text{P}_{680}^+$  on a time scale ranging from tens to few hundreds of nanoseconds, forming a  $\text{Y}_Z^\bullet$  radical; rapid proton release occurs upon the oxidation of  $\text{Y}_Z$  closely associated with the D1 residue His190 [5-7].  $\text{Y}_Z^\bullet$  reduction via electron transfer from the WOC occurs within the time interval of tens of microseconds to several milliseconds, depending on the S-state transitions of the WOC.

When the water-splitting complex is inactivated by removal of the  $\text{Mn}_4\text{CaO}_5$  cluster (apo-WOC-PS2), the electron transfer from  $\text{Y}_Z$  to  $\text{P}_{680}^+$  slows down. The pH-dependence of the reaction rate, deuterium kinetic isotope effects, and activation energies in the resulting complex differ significantly from those in the intact PS2 [4, 5]. The data obtained for apo-PS2 suggest that  $\text{Y}_Z$  resides in a solvent-exposed disordered environment [5, 7]. It is believed that changes in the dielectric properties increase the energy of reorganization and activation, which, in turn, decreases the electron transfer rate by 2-3 orders of magnitude relative to that in the active enzyme [4, 8-10]. Extraction of Mn ions from the WOC inhibits electron transfer from  $\text{Q}_A$  to  $\text{Q}_B$ , possibly,

by shifting the midpoint potential of  $Q_A$  to a more positive value [11-14]. Inhibition of the reaction on the RC acceptor side promotes electron recombination between  $Q_A^-$  and  $P_{680}^+$ .

The PS2 complex devoid of the  $Mn_4CaO_5$  cluster and three peripheral proteins is a convenient model for studying (i) the functional role of individual inorganic cofactors involved in the water oxidation, (ii) mechanisms of the inorganic core assembly (WOC photoactivation), (iii) mechanisms of the WOC reconstruction in the presence of various synthetic manganese compounds, (iv) the role of PS2 external proteins, (v) mechanisms of PS2 RC photoinhibition, (vi) the efficiency of exogenous electron donors and acceptors *in vitro*, etc.

The redox-active tyrosine  $Y_Z$  is commonly considered as a part of the single-electron “wiring” and not as a component of the pentametal  $Mn_4CaO_5$  cluster [4-6]. In this regard, it is important to know the nature of the  $Y_Z$  protein environment and the mechanisms of its interaction with water molecules and the manganese cluster of PS2. In this work, in order to reveal the properties of  $Y_Z$  functioning, we studied the effects of various low-molecular-weight compounds (sodium acetate, ammonium chloride, sodium formate, and sodium azide) on the electron transfer between  $Y_Z$  and  $P_{680}^+$  in the apo-PS2 complexes using optical pulse spectroscopy (measurement of absorbance changes at 830 nm) and direct electrometrical technique (measurement of light-induced photoelectric responses) [15, 16]. The obtained data indicate the two-phase electrogenic nature of the electron transfer between  $Y_Z$  and  $P_{680}^+$  that was significantly accelerated in the presence of sodium acetate and ammonium chloride.

## MATERIALS AND METHODS

**Spinach PS2 core complexes** were isolated from commercial spinach plants (*Spinacia oleracea*) as described by Haag et al. [17] by treatment of the membrane fragments with dodecyl- $\beta$ -D-maltoside [10 : 1, detergent/chlorophyll (Chl)] for 1 h followed by sucrose density centrifugation (20-40%) (Spinco L2 65B, SW-28 rotor) for 16 h at 4°C at 145,000g.

**To prepare manganese-depleted apo-PS2**, thawed intact PS2 core particles (0.5 mg Chl per ml) were incubated in the presence of 0.8 M Tris-HCl buffer (pH 8.3) for 30 min at 23°C followed by washing 3 times with the buffer (50 mM Mes-NaOH,

pH 6.0) [18].

**Liposomes** were produced from azolectin [20 mg/ml, type IVS, 40% (w/w) phosphatidylcholine content; Sigma] by sonication (at 22 kHz, 60  $\mu$ A) for 2 min in 50 mM HEPES-NaOH buffer, pH 7.5, containing 1.4% (w/v) *n*-octyl- $\beta$ -D-glucopyranoside. Reconstitution of protein complexes in proteoliposomes was carried out by mixing the liposomes with apo-PS2 at a lipid/protein ratio of 50 : 1 (w/w) for 30 min in the dark. The detergent was removed by filtration on a Sephadex G-50 column.

**Flash-induced absorption changes at 830 nm** were registered with a laboratory-built single-beam differential spectrophotometer. A laser diode with a wavelength of 830 nm was used as a measuring light source. Nd-YAG laser (Quantel, France) pulses were used as an actinic source of light (wavelength, 532 nm; full width at half maximum, 12 ns; flash intensity, 50 mJ).

**Generation of photoelectric response ( $\Delta\Psi$ )** was recorded by direct electrometrical technique as described in [16]. The transmembrane electric potential ( $\Delta\Psi$ ) generated on the vesicle membrane as a result of PS2 activity and then proportionately distributed to the measuring membrane was detected by the Ag/AgCl electrodes situated on the two sides of the membrane. A Quantel Nd-YAG laser was used as a source of light pulses.

**Signal kinetics were analyzed** using the program packages Pluk [19] and Origin (OriginLab Corporation, USA).

## RESULTS AND DISCUSSION

Photooxidized  $P_{680}$  in the Mn-depleted PS2 core complexes can be reduced in different ways: 1) by direct electron transfer from the redox-active tyrosine  $Y_Z$ ; 2) as a result of recombination of charges between  $P_{680}^+$  and the primary quinone acceptor  $Q_A^-$ ; 3) by the electron transfer from cytochrome  $b_{559}$  or tyrosine  $Y_D$  [10, 20]. As mentioned above,  $Y_Z$  is the main electron donor for  $P_{680}^+$  in such complexes; however,  $Y_Z$  is reduced as a result of recombination of the  $Y_Z \cdot Q_A^-$  charges and not by the electron from the manganese cluster. Since cytochrome  $b_{559}$  and/or tyrosine  $Y_D$  are in the oxidized form, the third mechanism of  $P_{680}^+$  reduction is unlikely in the apo-PS2 complexes [20].

Formation of the stable radical pair  $P_{680}^+ Q_A^-$  and kinetics of the electron transfer from  $Y_Z$  to  $P_{680}^+$  can be registered by measuring the flash-induced absorption changes at

830 nm ( $\Delta A_{830}$ ) which correspond to the  $P_{680}$  redox transitions [10, 21-23]. Figure 1 shows the kinetics of flash-induced absorption changes at 830 nm in the Mn-depleted PS2 core complexes incubated for 10 min in the dark in the absence (curve 1) and presence (curve 2) of 1 mM potassium ferricyanide at pH 6.0.

It is important to note that both the amplitude and the kinetics of the photoinduced optical signal at 830 nm virtually did not change in response to a series of 11-15 laser flashes, which indicated that the initial state of the reaction center  $Y_Z P_{680} Q_A$  fully regenerated during the dark interval between the flashes (5 s). This conclusion is consistent with the published data that the charge recombination between  $Y_Z \cdot$  and  $Q_A^-$  occurs within the time interval from several tens to several hundreds of milliseconds [7, 23, 24]. As can be seen from Fig. 1 (curve 2), the amplitude of the photo-induced  $\Delta A_{830}$  signal was 35% higher in the presence of 1 mM ferricyanide. This was most likely due to the fact that in some apo-PS2 RCs, the primary quinone acceptor  $Q_A$  initially was in the reduced state and, hence, the primary photoinduced pair  $P_{680}^+ Q_A^-$  did not form.

The relaxation kinetics reflecting  $P_{680}^+$  reduction was biphasic with characteristic times ( $\tau$ ) of  $\sim 7$  and  $\sim 31$   $\mu$ s and amplitudes of  $\sim 54$  and  $\sim 37\%$ , respectively (Fig. 1, curve 2, and table). These phases are indicative of the forward electron transfer from  $Y_Z$  to  $P_{680}^+$  [5, 10, 24] and suggest the presence of at least two distinct populations of PS2 centers differing by the interaction between  $Y_Z$  and D1-H190 (see below).

Figure 2 shows the effect of weak acids and  $NH_4Cl$  on the kinetics of electron transfer between  $Y_Z$  and  $P_{680}^+$  in the apo-PS2 complexes in solution (in the presence of 0.03% detergent). The effect of sodium acetate on the light-induced changes in the absorption at 830 nm corresponding to the oxidation (increase) and reduction (decrease) of  $P_{680}$  is demonstrated in Fig. 2a. Kinetic deconvolution of the  $\Delta A_{830}$  decay revealed its biphasic character with  $\tau_1$  of 5  $\mu$ s and  $\tau_2$  of 16  $\mu$ s in the presence of 50 mM acetate (curve 2) and with  $\tau_1$  of  $\sim 1$   $\mu$ s and  $\tau_2$  of  $\sim 7$   $\mu$ s in the presence of 200 mM acetate (curve 3). Therefore, the electron transfer from  $Y_Z$  to  $P_{680}^+$  accelerated with the increase in the acetate concentration (table).

The effect of  $NH_4Cl$  on the electron transfer on the apo-PS2 donor side is shown in Fig. 2b. Addition of 50 mM  $NH_4Cl$  accelerated the decay of the  $\Delta A_{830}$  signal (curve 2) characterized by  $\tau_1 \sim 4$   $\mu$ s and  $\tau_2 \sim 17$   $\mu$ s (table). As in the case of acetate, further increase in the  $NH_4Cl$  concentration in the suspension (curve 3) led to the increase in the rate of electron transfer from  $Y_Z$  to  $P_{680}^+$  (table). It should be noted that the addition of large concentration of  $NH_4Cl$  can produce side effects induced by  $Cl^-$  anions

generated by  $\text{NH}_4\text{Cl}$  dissociation. Such effects have been studied for the PS2 membrane fragments with functionally active WOC [25, 26]. Addition of NaCl at concentrations up to 400 mM did not affect the kinetics of the optical signal decay in PS2 complexes devoid of the manganese cluster and three peripheral proteins (Tris-HCl-treated samples) (data not shown). This suggests that the observed acceleration of the signal decay in the presence of  $\text{NH}_4\text{Cl}$  was due to the influence of ammonium (see below). Note that at the same rates of photooxidized  $\text{P}_{680}^+$  reduction by  $\text{Y}_Z$ , the relative contribution of the phases to the kinetics of  $\Delta\text{A}_{830}$  signal decay was different in the presence of sodium acetate and ammonium chloride (table). At present, we have no unambiguous explanation for this difference.

The effect of another weak acid, formate, on the  $\Delta\text{A}_{830}$  signal kinetics reflecting reduction of photooxidized  $\text{P}_{680}$  as a result of electron transfer from  $\text{Y}_Z$  is shown in Fig. 2c. The presence of 200 mM formate (curve 1) did not affect the kinetics of signal decay, while at the formate concentration of 250 mM, the decay was accelerated, but to a lesser extent (curve 2).

The addition of sodium azide to a concentration of 50 mM did not affect the kinetics and the amplitude of the  $\Delta\text{A}_{830}$  signal decay (Fig. 2d, curve 1), while at higher azide concentrations (100 mM), a significant decrease in the signal amplitude was observed without changes in the kinetics of decay (Fig. 2d, curve 2). It is likely that under these conditions,  $\text{P}_{680}^+$  reduction within the time interval between the flashes was incomplete.

The effect of the studied compounds on the forward electron transfer between  $\text{Y}_Z$  and photooxidized  $\text{P}_{680}$  in apo-PS2 was also studied using direct electrometrical technique. Figure 3a shows the photoelectric responses of apo-PS2 samples incorporated into liposomes and adsorbed on the phospholipid-impregnated collodion film. Light-dependent charge transfer in the RC is accompanied by the formation of the transmembrane electric potential difference. The negative sign of  $\Delta\Psi$  indicates that the donor side is located at the external surface of the proteoliposomal membrane [18, 27, 28]. Such asymmetric orientation (>90%) of apo-PS2 in liposomes allows to study the mechanism of interaction between  $\text{Y}_Z$  and exogenous compounds after a single turnover flash using direct electrometry. Laser flash results in  $\Delta\Psi$  generation due to the charge separation ( $\text{P}_{680}^+\text{Q}_\text{A}^-$ ) across the RC and electron transfer from the redox-active  $\text{Y}_Z$  to  $\text{P}_{680}^+$  in apo-PS2 samples. The observed decay of the photoelectric response is due to the charge recombination between  $\text{Q}_\text{A}^-$  and  $\text{Y}_Z^\bullet$  (Fig. 3a). Besides the fast unresolvable phase

of  $\Delta\Psi$  generation ( $P_{680}^+Q_A^-$ ), an additional millisecond electrogenic phase ( $\sim 17\%$  of the total amplitude) in the photoelectric response kinetics was observed. The latter phase is related to the electrogenic reduction of  $P_{680}^+$  by  $Y_Z$  (Fig. 3b, curve 1). Kinetic analysis of this additional electrogenic phase revealed components with  $\tau_1$  of  $\sim 1 \mu\text{s}$  and  $\tau_2$  of  $\sim 14 \mu\text{s}$  and equal contribution. The difference in the rates of  $Y_Z \rightarrow P_{680}^+$  reaction in the membrane-reconstituted apo-PS2 (electrometrical data) and apo-PS2 in the detergent solution (optical data) can be due to the effect of proteoliposome lipids that maintain the optimal structure of proteins ensuring their efficient functioning [28, 29]. Here, we would like to note that direct electrometric method allows not only to reveal the kinetics of individual electrogenic reactions in PS2 RC, but also to determine the distances between the redox centers [24, 28].

Addition of 250 mM  $\text{NH}_4\text{Cl}$  (Fig. 3b, curve 2) to the incubation medium resulted in changes in the kinetics of the additional submillisecond  $\Delta\Psi$  rising phase, which may be associated with a significant acceleration of the electron transfer rate between  $Y_Z$  and  $P_{680}^+$  in the proteoliposomes with apo-PS2. Similar effect was observed in the presence of 200 mM acetate (data not shown). If we assume that the kinetics of electron transfer is accelerated approximately by a factor of 5 (as in the case of apo-PS2 in solution in the presence of acetate or ammonium), then under similar conditions in proteoliposomes, the kinetic components with the characteristic times of 1 and 14  $\mu\text{s}$  can be much smaller, approximately 0.2 and 3  $\mu\text{s}$ , respectively. Kinetic analysis can reveal only the slow (3- $\mu\text{s}$ ) component (see insert). It should be noted that the time resolution of the direct electrometric technique is 0.20-0.25  $\mu\text{s}$ .

Therefore, the data obtained using direct electrometric technique confirm the presence of two kinetic components of the  $Y_Z \rightarrow P_{680}^+$  reaction that were observed in the microsecond time domain by the pulsed absorption spectroscopy based on the  $\Delta A_{830}$  signal.

A few words on the structural features of the studied system. Removal of the  $\text{Mn}_4\text{CaO}_5$  cluster does not result in any noticeable movement of the CP43, CP47, D1, D2 subunits or domains at the PS2 donor side, or in region of membrane-spanning helices, or at the PS2 acceptor side [30]; small changes in apo-PS2 are limited to residues in the vicinity of the  $\text{Mn}_4\text{CaO}_5$  cluster. It is also known that the properties of  $Y_Z$  in the apo-PS2 complexes could be different from those in active PS2 [4, 10, 18]. It is believed that in these preparations,  $Y_Z$  is located in a hydrophilic environment and is exposed to the bulk water. Some compounds, such as manganese, ascorbate, 1,5-

diphenylcarbazide, benzidine, hydroxylamine, hydrazine, as well as a number of redox mediators, such as N,N,N',N'-tetramethyl-*p*-phenylenediamine, 2,3,5,6-tetramethyl-*p*-phenylenediamine, 2,6-dichlorophenylindophenol and phenazine methosulfate, can act as electron donors to oxidized Y<sub>Z</sub> in manganese-depleted PS2 [28].

The following should be noted regarding compounds used in this study: acetate (CH<sub>3</sub>COO<sup>-</sup>) within the PS2 protein matrix binds to the non-heme iron on the acceptor side and between Y<sub>Z</sub> and Mn cluster on the donor side [26, 31]. Under these conditions, retardation of the electron transfer reactions between Q<sub>A</sub> and Q<sub>B</sub> and Y<sub>Z</sub><sup>•</sup> reduction (particularly, S<sub>2</sub>Y<sub>Z</sub><sup>•</sup> → S<sub>3</sub>Y<sub>Z</sub> transition) take place. The deceleration of the reaction on the RC acceptor side is probably due to the disturbance in the protonation of the twice-reduced Q<sub>B</sub> (Q<sub>B</sub><sup>2-</sup>). Analysis of the ability of acetate to access Y<sub>Z</sub><sup>•</sup> in apo-PS2 using the ESSEM data suggested the absence of coupling between Y<sub>Z</sub><sup>•</sup> and acetate [32]; however, this does not exclude the effect of acetate on the Y<sub>Z</sub>-His190 environment.

ELDOR-detected NMR along with computational studies showed that NH<sub>3</sub> (a substrate analogue) binds as a terminal ligand to the Mn<sub>4</sub>A ion *trans* to the O5 μ4 oxido bridge in NH<sub>4</sub>Cl-treated cyanobacterial PS2 core complex at pH 7.5 [33, 34]. It should be noted that at neutral and acidic pH values, NH<sub>4</sub>Cl exists mainly in the form of NH<sub>4</sub><sup>+</sup>, while the relatively hydrophobic part of the apo-PS2 protein (in particular, in the vicinity of Y<sub>Z</sub>) contains neutral NH<sub>3</sub> molecules [35, 36]. Based on the degree of protolysis in the reaction NH<sub>4</sub><sup>+</sup> + H<sub>2</sub>O → NH<sub>3</sub> + H<sub>3</sub>O<sup>+</sup>, the concentration of NH<sub>3</sub> in the assay medium was ~25 μM (the concentration of RCs in proteoliposomes and in solution in the optical measurements was ~0.04 and ~0.4 μM, respectively). In addition, the pK for NH<sub>4</sub>Cl (pK<sub>a</sub> 9.24) in the assay medium can be shifted toward the acidic values; therefore, the concentration of NH<sub>3</sub> can be even higher.

Addition of another small carbonic acid, formate, also slows down electron transfer between Q<sub>A</sub> and Q<sub>B</sub> and Y<sub>Z</sub><sup>•</sup> reduction (as in the case of acetate) [31]. Unlike CH<sub>3</sub>COO<sup>-</sup> and NH<sub>3</sub>, formate presumably binds in the vicinity of Arg294 in the D2 subunit and strongly affects the properties of Y<sub>D</sub>, as it was suggested based on the studies of Mn-depleted PS2-enriched membranes and PS2 core complexes using <sup>13</sup>C-formate and comparison of Y<sub>D</sub><sup>•</sup>/Y<sub>D</sub> FTIR spectra [37]. However, the effect of 250 mM formate on the kinetics of the ΔA<sub>830</sub> signal decay, although less pronounced than the effects of acetate or ammonium, indicates its involvement in the deprotonation in the Y<sub>Z</sub>-H190 segment.

The lack of the effect of azide/hydrazoic acid (N<sub>3</sub><sup>-</sup>/HN<sub>3</sub>) on the kinetics of

electron transfer on the apo-PS2 donor side cannot be unambiguously explained. It is possible that the  $N_3^-$  radical, which is an inhibitor of  $Y_Z \rightarrow Q_A$  electron transfer in Tris-treated PS2, is not produced at a single enzyme turnover [38].

It should be noted that despite that acetate, azide, and formate have similar  $pK$  values (4.75, 4.6, and 3.75, respectively), these compounds exhibit different impact on the kinetics of electron transfer on the RC donor side, namely between  $Y_Z$  and photooxidized  $P_{680}$ , while the effects of acetate ( $pK$  4.75) and ammonium chloride ( $pK_a$  9.24) are similar, which might be related to the structural features of these compounds.

As mentioned above, proton-coupled electron transfer from the redox-active  $Y_Z$  to photooxidized  $P_{680}$  is strongly slowed down by Mn depletion. One possible explanation for this phenomenon is the breakage of the  $Y_Z$ -H190 hydrogen bond upon Mn depletion. In PS2 with the assembled metal cluster, redox-active  $Y_Z$  and H190 are connected through a strong 2.4 Å-long hydrogen bond [3], whereas in apo-PS2, the length of this bond is 2.8 Å-long. In addition,  $Y_Z$  is involved in a much less ordered H-bond, and the its aromatic ring is more mobile in apo-PS2 [39, 40]. Because  $Y_Z$  is protonated in the reduced state and deprotonated in the oxidized state ( $Y_Z^\bullet$ ), its oxidation involves both electron and proton transfer. The rate of  $Y_Z$  oxidation increases with pH, with  $pK_a$  values of 8.3, 7.0, and 7.5 [7]. It was suggested that that at low pH, H190 is protonated and has to be deprotonated before it is able to accept a proton from  $Y_Z$ . Oxidation of  $Y_Z$  at low pH values could be explained by the fact that  $Y_Z^\bullet$  has multiple H-bonding partners [7, 41].

Hence,  $CH_3COO^-$  and  $NH_3$  accelerate  $P_{680}$  reduction in apo-PS2, probably, by accepting the phenol proton mobilized upon  $Y_Z$  oxidation [7, 41]. It was shown earlier [7] that small organic bases (e.g., imidazole and ethanolamine) which shift the  $pK_{red}$  value of  $Y_Z$  are able to chemically rescue the D1-H190 mutant of the cyanobacterium *Synechocystis* and to restore rapid  $P_{680}$  reduction by accepting the phenol proton. The acceleration of  $P_{680}^+$  reduction by substituted imidazoles, histidine, Tris, and 1,4-diazabicyclo[2.2.2]octane was also observed in Mn-depleted PS2 particles from the wild-type cyanobacteria [41].

The biphasic nature of the additional electrogenic phase ( $\tau_1 \sim 1 \mu s$  and  $\tau_2 \sim 14 \mu s$  at pH 6.0) in the kinetics of photoelectric response ( $\sim 17\%$  of the total electrogenic phase) (Fig. 3b, curve 1) suggests the existence of two RC populations, differing in the nature of interactions between  $Y_Z$  and H190. Unlike  $Y_D$ ,  $Y_Z$  is located in a more hydrophilic environment; a network of additional hydrogen bonds forms around  $Y_Z^\bullet$  in

manganese-depleted PS2 [39, 42-44]. Direct electrometry is a sensitive technique that allows to register the kinetics of the intraprotein charge transfer over a distance of 0.5 Å in the direction perpendicular to the membrane plane and to evaluate the relative contribution of individual electrogenic reactions (dielectrically weighted distances between cofactors) to the total  $\Delta\Psi$  [16, 24, 27]. Therefore, it should be noted that both components ( $\tau_1$  and  $\tau_2$ ) with an equal contribution to the additional electrogenic phase are due to the electrogenic vectorial electron transfer between  $Y_Z$  and  $P_{680}^+$ . Earlier, Hays et al. [7] suggested that the slower (submillisecond) phases of  $P_{680}^+$  reduction reflect D1-H190 deprotonation in the RC.

Concentration-dependent acceleration of the electron transfer between  $Y_Z$  and  $P_{680}^+$  in PS2 with inactive WOC in the presence of  $\text{CH}_3\text{COO}^-$  and  $\text{NH}_3$  (present work), as well as upon addition of organic bases, such as imidazole, histidine or ethanolamine [7, 41], argues in favor of the binding of these molecules near the  $Y_Z$ -H190 domain within the protein matrix. Apparently, all these compounds, which differ in molecular size and chemical structure, interact with  $Y_Z$  or H190 as proton acceptors. Therefore, the obtained results suggest that the enhanced proton-donating ability of  $Y_Z$  is responsible for the high rates of  $P_{680}^+$  reduction and manifestation of fundamental properties of the proton-coupled electron transfer in general.

Here, we demonstrated for the first time the biphasic kinetics of  $P_{680}^+$  reduction on the RC donor side using optical spectroscopy and direct electrometrical technique. The data obtained are important for understanding the mechanism of interactions between exogenous substances, including synthetic manganese-containing compounds, capable of water photolysis, and oxidized tyrosine  $Y_Z$  in the manganese-depleted PS2 complexes.

**Funding.** This work was supported by the Russian Science Foundation (project 17-14-01323) and the Russian Foundation for Basic Research (project AAAA-A19-119012990175-9) within the framework of the State Assignment “Chemical and Physical Mechanisms of Interaction of Intense Laser Radiation with Biological Systems”.

**Acknowledgements.** The authors are grateful to A. Yu. Semenov for critical discussion.

**Conflict of interest.** The authors declare no conflict of interest in financial or

any other sphere.

**Ethical approval.** This article does not contain any studies with human participants or animals performed by any of the authors.

## REFERENCES

1. Ferreira, K. N., Iverson, T. M., Maghlaoui, K., Barber, J., and Iwata, S. (2004) Architecture of the photosynthetic oxygen-evolving center, *Science*, **303**, 1831-1838; doi: 10.1126/science.1093087.
2. Guskov, A., Kern, J., Gabdulkhakov, A., Broser, M., Zouni, A., and Saenger, W. (2009) Cyanobacterial photosystem II at 2.9-Å resolution and the role of quinones, lipids, channels and chloride, *Nat. Struct. Mol. Biol.*, **16**, 334-342; doi: 10.1038/nsmb.1559.
3. Umena, Y., Kawakami, K., Shen, J.-R., and Kamiya, N. (2011) Crystal structure of oxygen-evolving photosystem II at a resolution of 1.9 Å, *Nature*, **473**, 55-60; doi: 10.1038/nature09913.
4. Tommos, C., and Babcock, G. T. (2000) Proton and hydrogen currents in photosynthetic water oxidation, *Biochim. Biophys. Acta*, **1458**, 199-219; doi: 10.1016/S0005-2728(00)00069-4.
5. Renger, G. (2004) Coupling of electron and proton transfer in oxidative water cleavage in photosynthesis, *Biochim. Biophys. Acta*, **1655**, 195-204; doi: 10.1016/j.bbabi.2003.07.007Get.
6. Styring, S., Sjöholm, J., and Mamedov, F. (2012) Two tyrosines that changed the world: interfacing the oxidizing power of photochemistry to water splitting in photosystem II, *Biochim. Biophys. Acta*, **1817**, 76-87; doi: 10.1016/j.bbabi.2011.03.016.
7. Hays, A. M., Vassiliev, I. R., Golbeck, J. H., and Debus, R. J. (1999) Role of D1-His190 in the proton-coupled oxidation of tyrosine Y<sub>Z</sub> in manganese-depleted photosystem II, *Biochemistry*, **38**, 11851-11865; doi: 10.1021/bi990716a.
8. Babcock, G. T., and Sayer, K. (1975) A rapid, light-induced transient in electron paramagnetic resonance signal II activated upon inhibition of photosynthetic oxygen evolution, *Biochim. Biophys. Acta*, **376**, 315-328; doi: 10.1016/0005-2728(75)90024-9.

9. Conjeaud, H., and Mathis, P. (1980) The effects of pH on the reductions kinetics of P-680 in Tris-treated chloroplasts, *Biochim. Biophys. Acta*, **590**, 353-359; doi: 10.1016/0005-2728(80)90206-6.
10. Buser, C. A., Thompson, L. K., Diner, B. A., and Brudvig, G. W. (1990) Electron-transfer reactions in manganese-depleted photosystem II, *Biochemistry*, **29**, 8977-8985; doi: 10.1021/bi00490a014.
11. Krieger, A., Rutherford, A. W., and Johnson, G. N. (1995) On the determination of redox midpoint potential of the primary quinone electron acceptor,  $Q_A$ , in photosystem II, *Biochim. Biophys. Acta*, **1229**, 193-201; doi: 10.1016/0005-2728(95)00002-Z.
12. Shibamoto, T., Kato, Y., Sugiura, M., and Watanabe, T. (2009) Redox potential of the primary plastoquinone electron acceptor  $Q_A$  in photosystem II from *Thermosynechococcus elongatus* determined by spectroelectrochemistry, *Biochemistry*, **48**, 10682-10684; doi: 10.1021/bi901691j.
13. Ido, K., Gross, G. M., Guerrero, F., Sedoud, A., Lai, T. L., Ifuku, K., Rutherford, A. W., and Krieger-Liszkay, A. (2011) High and low potential forms of the  $Q_A$  quinone electron acceptor in photosystem II of *Thermosynechococcus elongatus* and spinach, *J. Photochem. Photobiol. B*, **104**, 154-157; doi: 10.1016/j.jphotobiol.2011.02.010.
14. Allakhverdiev, S. I., Tsuchiya, T., Watabe, K., Kojima, A., Los, D. A., Tomo, T., Klimov, V. V., and Mimuro, M. (2011) Redox potentials of primary electron acceptor quinone molecule ( $Q_A^-$ ) and conserved energetics of photosystem II in cyanobacteria with chlorophyll *a* and chlorophyll *d*, *Proc. Natl. Acad. Sci. USA*, **108**, 8054-8058; doi: 10.1073/pnas.1100173108.
15. Drachev, L. A., Jasaitis, A. A., Kaulen, A. D., Kondrashin, A. A., Liberman, E. A., Nemecek, I. B., Ostroumov, S. A., Semenov, A. Y., and Skulachev, V. P. (1974) Direct measurement of electric current generation by cytochrome oxidase,  $H^+$ -ATPase and bacteriorhodopsin, *Nature*, **249**, 321-324; doi: 10.1038/249321a0.
16. Drachev, L. A., Kaulen, A. D., Semenov, A. Yu., Severina, I. I., and Skulachev, V. P. (1979) Lipid-impregnated filters as a tool for studying the electric current-generating proteins, *Anal. Biochem.*, **96**, 250-262; doi: 10.1016/0003-2697(79)90580-3.
17. Haag, E., Irrgang, K.-D., Boekema, E. J., and Renger, G. (1990) Functional and structural analysis of photosystem II core complexes from spinach with high

- oxygen evolution capacity, *Eur. J. Biochem.*, **189**, 47-53; doi: 10.1111/j.1432-1033.1990.tb15458.x.
18. Gupta, O. A., Tyunyatkina, A. A., Kurashov, V. N., Semenov, A. Y., and Mamedov, M. D. (2008) Effect of redox mediators on the flash-induced membrane potential generation in Mn-depleted photosystem II core particles, *Eur. Biophys. J.*, **37**, 1045-1050; doi: 10.1007/s00249-007-0231-6.
  19. Kalaidzidis, Ya. L., Gavrilov, A. V., Zaitsev, P. V., Kalaidzidis, A. L., and Korolev, E. V. (1997) PLUK – an environment for software development, *Program Comput. Softw.*, **23**, 206-212.
  20. Kaminskaya, O., Kurreck, J., Irrgang, K. D., Renger, G., and Shuvalov, V. A. (1999) Redox and spectral properties of cytochrome  $b_{559}$  in different preparations of photosystem II, *Biochemistry*, **38**, 16223-16235; doi: 10.1007/s00249-015-1082-1.
  21. Van Best, J. A., and Mathis, P. (1978) Apparatus for the measurement of small absorption change kinetics at 820 nm in the nanosecond range after a ruby laser flash, *Rev. Sci. Instrum.*, **49**, 1332; doi: 10.1063/1.1135579.
  22. Renger, G., Volker, M., and Weiss, W. (1984) Studies on the nature of the water-oxidizing enzyme. I. The effect of trypsin on the system II reaction pattern in inside-out thylakoids, *Biochim. Biophys. Acta*, **766**, 582-591; doi: 10.1016/0005-2728(84)90118-X.
  23. Gadjieva, R., Eckert, H.-J., and Renger, G. (2000) Photoinhibition as a function of the ambient redox potential in Tris-washed PS II membrane fragments, *Photosynth. Res.*, **63**, 237-248; doi: 10.1023/A:1006427408083.
  24. Semenov, A., Cherepanov, D., and Mamedov, M. (2008) Electrogenic reactions and dielectric properties of photosystem II, *Photosynth. Res.*, **98**, 121-130; doi: 10.1007/s11120-008-9377-z.
  25. Tsuno, M., Suzuki, H., Kondo, T., Mino, H., and Noguchi, T. (2011) Interaction and inhibitory effect of ammonium cation in the oxygen evolving center of photosystem II, *Biochemistry*, **50**, 2506-2514; doi: 10.1021/bi101952g.
  26. Lovyagina, E. R., and Semin, B. K. (2016) Mechanism of inhibition and decoupling of oxygen evolution from electron transfer in photosystem II by fluoride, ammonia and acetate, *J. Photochem. Photobiol. B*, **158**, 145-153; doi: 10.1016/j.jphotobiol.2016.02.031.

27. Haumann, M., Mulikidjanian, A., and Junge, W. (1997) Electrogenicity of electron and proton transfer at the oxidizing side of photosystem II, *Biochemistry*, **36**, 9304-9315; doi: 10.1021/bi963114p.
28. Mamedov, M. D., Kurashov, V. N., Cherepanov, D. A., and Semenov, A. Yu. (2010) Photosystem II: where does the light-induced voltage come from? *Front. Biosci.*, **15**, 1007-1017; doi: 10.2741/3658.
29. Petrova, I. O., Kurashov, V. N., Semenov, A. Yu., and Mamedov, M. D. (2011) Mn-depleted/reconstituted photosystem II core complexes in solution and liposomes, *J. Photochem. Photobiol. B*, **104**, 372-376; doi: 10.1016/j.jphotobiol.2011.03.004.
30. Zhang, M., Bommer, M., Chatterjee, R., Hussein, R., Yano, J., Dau, H., Kern, J., Dobbek, H., and Zouni, A. (2017) Structural insights into the light-driven auto-assembly process of the water-oxidizing Mn<sub>4</sub>CaO<sub>5</sub>-cluster in photosystem II, *eLife*, **6**, e26933; doi: 10.7554/eLife.26933.
31. Shevela, D., Klimov, V., and Messinger, J. (2007) Interactions of photosystem II with bicarbonate, formate and acetate, *Photosynth. Res.*, **94**, 247-264; doi: 10.1007/s11120-007-9200-2.
32. Clemens, K. L., Force, D. A., and Britt, R. D. (2002) Acetate binding at the photosystem II oxygen-evolving complex: an S<sub>2</sub>-state multiline signal ESEEM study, *J. Am. Chem. Soc.*, **124**, 10921-10933; doi: 10.1021/ja012036c.
33. Hou, L.-H., Wu, C.-M., Huang, H.-H., and Chu, H.-A. (2011) Effects of ammonia on the structure of the oxygen-evolving complex in photosystem II as revealed by light-induced FTIR difference spectroscopy, *Biochemistry*, **50**, 9248-9254; doi: 10.1021/bi200943q.
34. Marchiori, D. A., Oyala, P. H., Debus, R. J., Stich, T. A., and Britt, R. D. (2018) Structural effects of ammonia binding to the Mn<sub>4</sub>CaO<sub>5</sub> cluster of photosystem II, *J. Phys. Chem. B*, **122**, 1588-1599; doi: 10.1021/acs.jpcc.7b11101.
35. Gerhard, V. (1980) The effect on ammonium chloride on the kinetics of the back reaction of photosystem II in *Chlorella fusca* and in chloroplasts in the presence of 3-(3,4-dichlorophenyl)-1,1-dimethylurea, *Z. Naturforsch.*, **35**, 451-460; doi: 10.1515/znc-1980-5-616.
36. Kleiner, D. (1981) The transport of NH<sub>3</sub> and NH<sub>4</sub><sup>+</sup> across biological membranes, *Biochim. Biophys. Acta*, **639**, 41-52; doi: 10.1016/0304-4173(81)90004-5.

37. Hienerwadel, R., Gourion-Arsiquaud, S., Ballottari, M., Bassi, R., Diner, B. A., and Berthomieu, C. (2005) Formate binding near the redox-active tyrosine D in photosystem II: consequences on the properties of tyrD, *Photosynth. Res.*, **84**, 139-144; doi: 10.1007/s11120-005-0637-x.
38. Kawamoto, K., Mano, J., and Asada, K. (1995) Photoproduction of the azidyl radical from the azide anion on the oxidizing side of photosystem II and suppression of photooxidation of tyrosine Z by the azidyl radical, *Plant Cell Physiol.*, **36**, 1121-1129; doi: 10.1093/oxfordjournals.pcp.a078856.
39. Force, D. A., Randall, D. W., Britt, R. D., Tang, X. S., and Diner, B. A. (1995) 2H ESE-ENDOR study of hydrogen bonding to the tyrosine radicals  $Y_D^{\bullet}$  and  $Y_Z^{\bullet}$  of photosystem II, *J. Am. Chem. Soc.*, **117**, 10547-10554; doi: 10.1021/ja00155a032.
40. Tommos, C., Tang, X. S., Warncke, K., Hoganson, C. W., Styring, S., McCracken, J., Diner, B. A., and Babcock, G. T. (1995) Spin-density distribution, conformation, and hydrogen bonding of the redox-active tyrosine  $Y_Z$  in photosystem II from multiple-electron magnetic-resonance spectroscopies: implications for photosynthetic oxygen evolution, *J. Am. Chem. Soc.*, **117**, 10325-10335; doi: 10.1021/ja00146a017.
41. Hays, A. M., Vassiliev, I. R., Golbeck, J. H., and Debus, R. J. (1998) Role of D1-His190 in proton-coupled electron transfer reactions in photosystem II: a chemical complementation study, *Biochemistry*, **37**, 11352-11365; doi: 10.1021/bi980510u.
42. Berthomieu, C., Hienerwadel, R., Boussac, A., Breton, J., and Diner, B. (1998) Hydrogen bonding of redox-active tyrosine Z of photosystem II probed by FTIR difference spectroscopy, *Biochemistry*, **37**, 10547-10554; doi: 10.1021/bi980788m.
43. Diner, B. A., Force, D. A., Randall, D. W., and Britt, R. D. (1998) Hydrogen bonding, solvent exchange, and coupled proton and electron transfer in the oxidation and reduction of redox-active tyrosine  $Y_Z$  in Mn-depleted core complexes of photosystem II, *Biochemistry*, **37**, 17931-17943; doi: 10.1021/bi981894r.
44. Campell, K. A., Peloquin, J. M., Diner, B. A., Tang, X. S., Chisholm, D. A., and Britt, R. D. (1997) The  $\tau$ -nitrogen of D2 histidine 189 is the hydrogen bond donor to the tyrosine radical  $Y_D^{\bullet}$  of photosystem II, *J. Am. Chem. Soc.*, **119**, 4787-4788; doi: 10.1021/ja9706155.

Effect of ammonium acetate and ammonium chloride on the recombination kinetics of the  $\Delta A_{830}$  signal

Concentration, mM	CH <sub>3</sub> COONa		NH <sub>4</sub> Cl	
	Time, $\mu$ s	Amplitude, %	Time, $\mu$ s	Amplitude, %
25	5	58	–	–
	17	34		
50	5	74	4	36
	16	22	17	54
100	1	60	6	27
	9	35	13	62
200	1	70	1.4	27
	7	23	9	62
250	–		1.3	32
			7	59

Note: The data are presented for control samples (without additions) with two kinetic components with characteristic times  $\tau_1 \sim 7 \mu$ s and  $\tau_2 \sim 31 \mu$ s and relative contribution of  $\sim 54$  and  $37\%$ , respectively. The time ( $\mu$ s) reflects the rates of photooxidized P<sub>680</sub> reduction by Y<sub>Z</sub>, and the amplitude of individual kinetic phases (%) reflects relative phase contribution to the kinetics of optical signal decay.

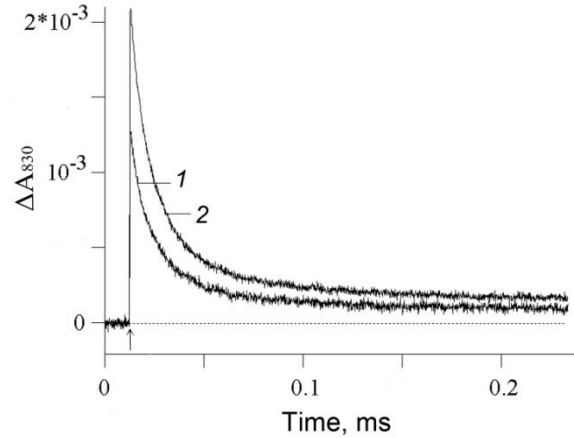


**Fig. 1.** Absorption changes at 830 nm in apo-PS2 complexes induced by non-saturating laser flashes corresponding to the oxidation (increase) and reduction (decrease) of  $P_{680}$  in the absence (1) and presence (2) of 1 mM potassium ferricyanide. Chl concentration, 20  $\mu\text{g/ml}$ ; time interval between single turnover flashes, 5 s. Each curve was averaged from 11-15 traces. Incubation medium: 50 mM Mes-NaOH, pH 6.0, 15 mM NaCl, 0.35 M sucrose, 0.025% dodecyl maltoside (w/v). Here and below, arrows indicate the moments of laser flashes.

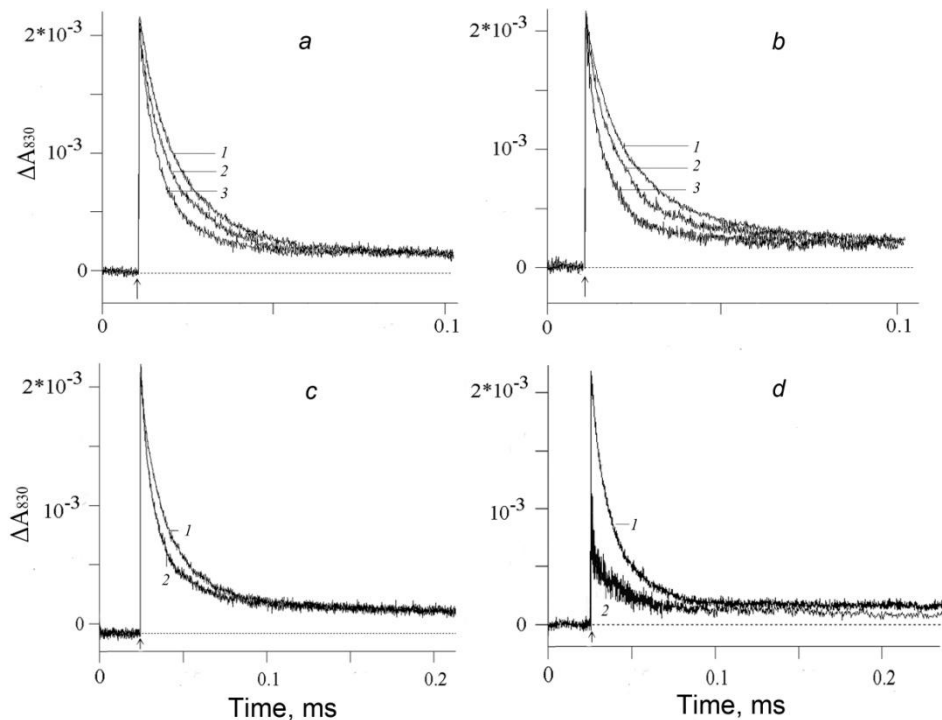


**Fig. 2.** Changes in the absorption at 830 nm in the apo-PS2 complexes induced by non-saturating laser flashes: a) in the absence (1) and presence of 50 mM (2) and 200 mM (3) sodium acetate; b) in the absence (1) and presence of 50 mM (2) and 250 mM (3)  $\text{NH}_4\text{Cl}$ ; c) in the presence of 200 mM (1) and 250 mM (2) sodium formate; d) in the presence of 50 mM (1) and 100 mM (2) sodium azide. Conditions as in Fig. 1.

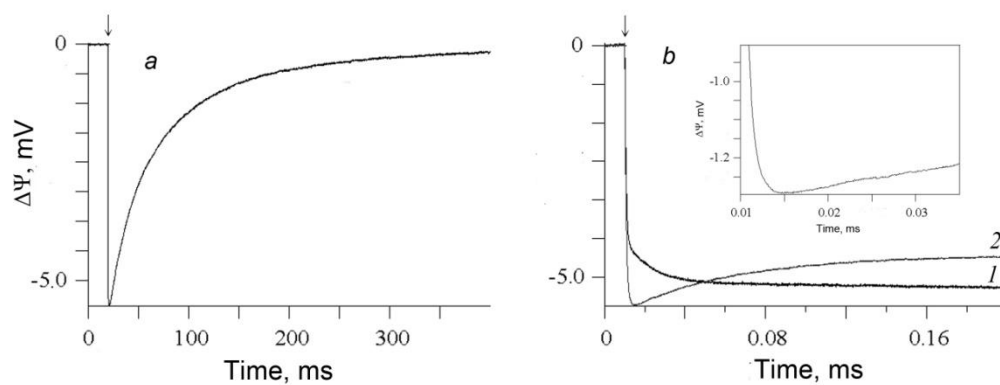


**Fig. 3.** a) Flash-induced photoelectric response in proteoliposomes containing apo-PS2 complexes. b) Photoelectric responses in the absence (1) and presence of 250 mM  $\text{NH}_4\text{Cl}$  (2). Insert, enlarged initial fragment of curve (2) showing the fast phase. Conditions as in Fig. 1.